A DHT-Based Multicarrier Modulation System with Pairwise ML Detection

Juquan Mao[1], Chin-Liang Wang[21], Lei Zhang [3], Chang He[1], Pei Xiao[1], Konstantinos Nikitopoulos[1]
[1] 5G Innovation Center, Institute for Communication Systems, University of Surrey, GU2 7XH, UK
{juquan.mao, c.he, p.xiao, k.nikitopoulos}@surrey.ac.uk
[2] Department of Electrical Engineering, National Tsing Hua University, Hsinchu 30013, Taiwan
clwang@ee.nthu.edu.tw
[3] Lei Zhang, School of Engineering, University of Glasgow, Glasgow, G12 8QQ, UK
lei.zhang@glasgow.ac.uk

This paper presents a complex-valued discrete multicar- rier modulation (MCM) system based on the real-valued discrete Hartley transform (DHT) and its inverse (IDHT). Unlike the conventional discrete Fourier transform (DFT), the DHT can not diagonalize multipath fading channels due to its inherent properties, and this results in mutual interference between subcarriers of the same mirror- symmetrical pair. We explore this interference pattern in order to seek an optimal solution to utilize channel diversity for enhancing the bit error rate (BER) perfor- mance of the system. It is shown that the optimal channel diversity gain can be achieved via pairwise maximum likelihood (ML) detection, taking into account not only the subcarrier's own channel quality but also the channel state information of its mirror-symmetrical peer. Performance analysis indicates that DHT-based MCM can mitigate fast fading effect by averaging channel power gains on each mirror-symmetrical pair of subcarriers. Simulation results show that the scheme has a substantial improvement in BER over the conventional DFT-based MCM system.

Index Terms**—discrete Hartley transform, multicarrier modulation, Diversity, Maximum Likelihood Detection**

I. Introduction

Multi-carrier modulation (MCM) technique, pre- sented as an elegant solution to combat inter-symbol interference (ISI) [1], has been widely adopted for air interfaces of many wireless systems and is considered as a candidate for the next-generation of cellular systems. Orthogonal frequency-division multiplexing (OFDM) is a dominant approach in MCM where complex expo- nential functions form an orthogonal basis. In OFDM systems, digital baseband modulation and demodulation can be implemented with fast algorithms of the inverse discrete Fourier transform (IDFT) and DFT [2] respec- tively, namely inverse fast Fourier transform (IFFT) and FFT algorithms. Due to this important feature, OFDM has been widely used in various systems including the fourth generation (4G) and the fifth generation (5G) [3], [4]. Note that, the complex exponential functions set is not the only orthogonal basis to construct baseband multicarrier signals. A set of sinusoidal and cosinusoidal functions can be exploited as an alternative orthogonal basis to implement an MCM scheme [5]–[8], where signals can be synthesized with the discrete Hartley transform (DHT). Hereafter we denote the scheme as DHT-based MCM. It is shown later that DHT-based MCM can utilize channel diversity gain to achieve bet- ter system performance. It is also worth mentioning that the existing fast Hartley transform (FHT) algorithms, such as those in [9], [10] can be employed for a fast implementation of the scheme.

This work was supported by the Royal Society of the United Kingdom under Grant IE150103 as well as by the Ministry of Science and Technology of Taiwan, R.O.C., under Grant MOST 105-2221-E-007-018-MY2.

A DHT-based MCM scheme was initially proposed for transmitting real-valued signals in wireline systems [7], [11]. The authors in [12] also proposed a DHT- based MCM for ultra-band system. Two issues hin- der these schemes to be applied to wireless systems. First, they halve the spectrum efficiency of conventional OFDM as only one-dimensional modulation schemes such as M-ary pulse amplitude modulation (PAM) are supported. Second, the inherent inter-carrier inter- ference (ICI) due to non-diagonal channel response matrix degrades system performance. To combat these issues, Jao et al. proposed a DHT-based system in [8], which not only transmits 2-D complex symbols but also eliminates ICI effects by adding linear transform blocks on the transmitter and receiver to diagonalize the fre- quency domain channel response matrix. In this paper we propose a generalized DHT-based MCM transceiver structure to achieve channel diversity gain without adding any additional functional blocks. DHT transform can not diagonalize the multipath fading channel, which resulting in the mutual interference between subcarriers in the same mirror-symmetrical pair. We explore the
interference pattern and decouple the channel matrix

into pairs of mirror-symmetric subcarriers. The ML detection is then applied to each pair not only to eliminate the inherent ICI but also to explore subcarrier channel diversity resulting an improved BER over other DFT-based MCM systems.

The rest of this paper is organized as follows. Section II describes a generalized MCM system model under consideration and also discusses the properties of DFT- based and DHT-based MCM systems. In Section III, we propose a DHT-based transceiver system and present the corresponding pairwise ML detection at the receiver side. Simulation results are given in Section IV, and the conclusion is finally drawn in Section V.

II. System Model

Consider a general discrete N-point multicarrier sys- tem, where $\mathbf{Q}_T$ and $\mathbf{R}_T$ are the transmitter and receiver side transforms respectively such that $\mathbf{Q}_T\mathbf{R}_T = \mathbf{I}$. Let $\mathbf{X} = [X_0, X_1, ..., X_{N-1}]^T$ be an $N \times 1$ frequency-domain symbol vector generated from a bit-to-symbol demapper, where $[.]^T$ denotes transpose operation. The transmitter side transform $\mathbf{Q}_T$ is applied to this symbol vector to obtain an $N \times 1$ time domain sample vector $\mathbf{x} = \mathbf{Q}_T\mathbf{X}$.

A cyclic prefix (CP) of P-samples is then appended to the vector $\mathbf{x}$ and is transmitted over an L-path frequency selective channel, where P is greater than L to ensure free inter-symbol interference (ISI). After removing the CP, the received symbol vector can be expressed as

$$\mathbf{y} = \mathbf{A}_c\mathbf{x} + \mathbf{v}, \tag{1}$$

where $\mathbf{A}_c$ is the $N \times N$ circulant channel matrix with its $(k, \underline{k})^{th}$ entry given as $\mathbf{A}_c(k, \underline{k}) = h(k - \underline{k} \mod N)$ such that $h(i)$, $0 \le i \le L-1$ is the i^{th} tap of channel impulse response (CIR); $\mathbf{v}$ is an $N \times 1$ addictive white Gaussian noise (AWGN) vector with zero mean and variance of N_0.

At the receiver side, the received symbol vector is transformed by $\mathbf{R}_T$ to obtain a frequency-domain symbol vector given as

$$\mathbf{Y} = \mathbf{R}_T\mathbf{A}_c\mathbf{Q}_T\mathbf{X} + \mathbf{v}^i, \tag{2}$$

where $\mathbf{v}^i = \mathbf{R}_T\mathbf{v}$. If $\mathbf{A}_c$ can be diagonalized by $\mathbf{R}_T$ and $\mathbf{Q}_T$, or $\mathbf{R}_T\mathbf{A}_c\mathbf{Q}_T$ is a diagonal matrix, a linear frequency domain equalizer (FDE) $\mathbf{E}$ can be employed to estimate the transmitted vector

$$\begin{aligned}\hat{\mathbf{X}} &= \mathbf{E}\mathbf{Y}\\ &= \mathbf{X} + \mathbf{E}\mathbf{v}^i.\end{aligned} \tag{3}$$

Otherwise, linear equalizations don't present an optimal solution and non-linear equalizations need to be consid- ered in order to maximum system BEP.

A. DFT Property

Consider DFT based OFDM system where the matri- ces $\mathbf{Q}_T$ and $\mathbf{R}_T$ are IDFT matrix $\mathbf{F}$ and DFT matix $\mathbf{F}^H$ respectively and $[.]^H$ denotes the conjugates transpose operation. The $(n, k)^{th}$ entry of IDFT matrix is defined as

$$\mathbf{F}(n, k) = \frac{1}{\sqrt{N}} \exp\left(\frac{j2\pi nk}{N}\right), \qquad 0 \le n, k \le N-1. \tag{4}$$

According to the property of circulant matrices in [13], the received symbol vector in the frequency domain in (2) can be rewritten as

$$\mathbf{Y} = \mathbf{F}\mathbf{A}_c\mathbf{F}^H\mathbf{X} + \mathbf{v}^i = \mathbf{\Lambda}\mathbf{X} + \mathbf{v}^i \tag{5}$$

where

$$\mathbf{\Lambda} = \mathbf{F}\mathbf{A}_c\mathbf{F}^H = \mathrm{diag}\{\lambda_k\}, \ 0 \le i \le N-1 \tag{6}$$

is the diagonal matrix whose diagonal elements are the DFT coefficients of the circulant channel matrix $\mathbf{A}_c$. In such case, one-tap zero-forcing (ZF) equalization can be applied on a subcarrier basis given as

$$\hat{X}_i = \frac{Y_i}{\lambda_i} = x_i + \frac{v_i^i}{\lambda_i}. \tag{7}$$

B. DHT Property and Problem Definition

DHT and IDHT have an identical transform Matrix $\mathbf{H}$, the DHT of a real sequence $\mathbf{d} = [d_0, d_1, ..., d_{N-1}]^T$ and its inverse are defined as

$$\begin{aligned} D_n &= \frac{1}{\sqrt{N}}\sum_{k=0}^{N-1} d_k \mathrm{cas}\left(\frac{2\pi kn}{N}\right), \quad 0 \le n \le N-1\\ d_k &= \frac{1}{\sqrt{N}}\sum_{n=0}^{N-1} D_n \mathrm{cas}\left(\frac{2\pi kn}{N}\right), \quad 0 \le k \le N-1 \end{aligned} \tag{8}$$

where

$$\mathrm{cas}\, x \equiv \cos x + \sin x.$$

By denoting the $(n, k)^{th}$ entries of $N \times N$ matrices $\mathbf{C}$ and $\mathbf{S}$ as

$$\begin{aligned} \mathbf{C}(n, k) &= \frac{1}{\sqrt{N}} \cos\left(\frac{2\pi nk}{N}\right)\\ \mathbf{S}(n, k) &= \frac{1}{\sqrt{N}} \sin\left(\frac{2\pi nk}{N}\right), \quad 0 \le n, k \le N-1, \end{aligned} \tag{9}$$

the DFT and DHT matrices can be written as

$$\mathbf{F} = \mathbf{C} + j\mathbf{S} \tag{10}$$

$$\mathbf{H} = \mathbf{C} + \mathbf{S}. \tag{11}$$

According to (5) the circulant matrices can be diag- onalized by using DFT transform. Here, we investigate whether the DHT matrix has the same property. To ease the investigation, we let $\mathbf{A}_c$ be a real-valued matrix now

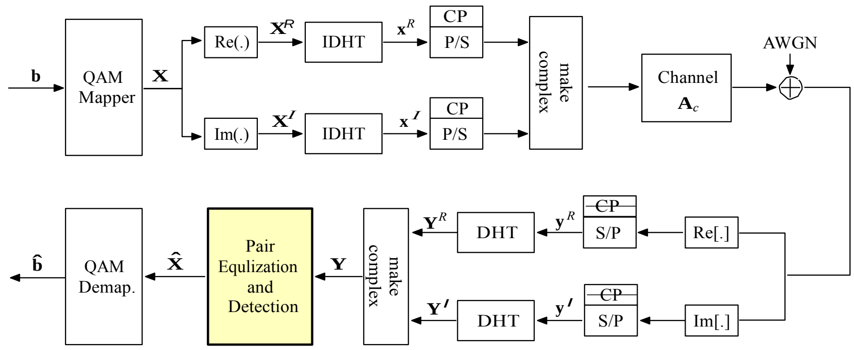

Fig. 1. Block diagram of the proposed DHT-based MCM scheme.

and extend it to complex-valued in the next section. Substituting (10) into (6), we have

$$\boldsymbol{\Lambda} = (\mathbf{SA}_c\mathbf{S} + \mathbf{CA}_c\mathbf{C}) + \boldsymbol{j}(\mathbf{CA}_c\mathbf{S} - \mathbf{SA}_c\mathbf{C}), \quad (12)$$

where

$$\begin{aligned} \mathrm{Re}\{\boldsymbol{\Lambda}\} &= \mathbf{SA}_c\mathbf{S} + \mathbf{CA}_c\mathbf{C} \\ \mathrm{Im}\{\boldsymbol{\Lambda}\} &= \mathbf{CA}_c\mathbf{S} - \mathbf{SA}_c\mathbf{C} \end{aligned} \quad (13)$$

Now replacing the transmitter and receiver side transforms $\mathbf{Q}_T$ and $\mathbf{R}_T$ in (2) with the DHT matrix $\mathbf{H}$, we have

$$\begin{aligned} \mathbf{HA}_c\mathbf{H} &= (\mathbf{C} + \mathbf{S})\mathbf{A}_c(\mathbf{C} + \mathbf{S}) \\ &= \mathbf{SA}_c\mathbf{S} + \mathbf{CA}_c\mathbf{C} + \mathbf{CA}_c\mathbf{S} + \mathbf{SA}_c\mathbf{C}. \end{aligned} \quad (14)$$

According to [8], the following equation holds:

$$\mathbf{CA}_c\mathbf{S} + \mathbf{SA}_c\mathbf{C} = \mathbf{J}_N(\mathbf{CA}_c\mathbf{S} - \mathbf{SA}_c\mathbf{C}), \quad (15)$$

where $\mathbf{J}_n$ is defined as

$$\mathbf{J}_N = \begin{bmatrix} 1 & 0 & \cdots & \cdots & 0 \\ 0 & & & \iddots & 1 \\ \vdots & & \iddots & \iddots & 0 \\ \vdots & \iddots & \iddots & \iddots & \vdots \\ 0 & 1 & 0 & \cdots & 0 \end{bmatrix}.$$

Substituting (13) and (15) into (14), one can obtain

$$\begin{aligned} \mathbf{HA}_c\mathbf{H} &= \mathrm{Re}\{\boldsymbol{\Lambda}\} + \mathbf{J}_n\mathrm{Im}\{\boldsymbol{\Lambda}\} \\ &= \begin{bmatrix} \mathrm{Re}\{\lambda_0\} & 0 & \cdots & \cdots & 0 \\ 0 & \mathrm{Re}\{\lambda_1\} & & & \mathrm{Im}\{\lambda_{N-1}\} \\ \vdots & & \ddots & \iddots & \\ \vdots & & \iddots & \ddots & \\ 0 & \mathrm{Im}\{\lambda_1\} & & & \mathrm{Re}\{\lambda_{N-1}\} \end{bmatrix}. \end{aligned} \quad (16)$$

Eq. (16) indicates the DHT transform can not diagonalize the circulant matrix $\mathbf{A}_c$ but will result in a sparse matrix with the non-zero main diagonal entries $\mathrm{Re}\{\lambda_0, \lambda_1, \ldots, \lambda_{N-1}\}$ and first anti-diagonal entries $\mathrm{Im}\{\lambda_1, \lambda_2, \ldots, \lambda_{N-1}\}$ below the zero main anti-diagonal entries. Consequently, for an MCM system with real-valued CIR, the transmitted symbols on mirror-symmetric subcarriers couple together and induce inter-carrier interference (ICI) if the DHT-based multicarrier modulator is employed. In order to tackle ICI, one previous work in [12] arranges conjugated symbols on mirror-symmetric subcarriers to achieve subcarrier diversity gain at a cost of half data rate.

III. Proposed DHT-Based MCM System

In this section, we propose a DHT-based MCM transceiver system using two real-valued DHT modules to transform real and imaginary parts of M-ary QAM symbols respectively, as shown in Fig. 1. In addition, a novel equalization and detection method is proposed to eliminate the ICI between mirror-symmetric subcarriers.

A. System Description

A sequence of encoded or raw bits $\mathbf{b}$ is fed into a M-ary QAM demapper to generate a complex symbol vector $\mathbf{X}$ of which each element $X_i \in S = \{s_0, s_1, \ldots, s_{M-1}\}$, $0 \leq i \leq N-1$. $\mathbf{X}$ is then divided into two vectors $\mathbf{X}^R$ and $\mathbf{X}^I$ corresponding to the real part and the imaginary part of $\mathbf{X}$. Following the same procedure described in Section II, we can replace the transmitter and receiver side transforms $\mathbf{Q}_T$ and $\mathbf{R}_T$ with DHT matrix $\mathbf{H}$ for parallel transmission of $\mathbf{X}^R$ and $\mathbf{X}^I$ respectively. After DHT at the receiver side, according to (2), the received complex symbol vector in the frequency domain can be expressed as

$$\begin{aligned} \mathbf{Y} &= \mathbf{HA}_c\mathbf{HX} + \mathbf{v}^i \\ &= \mathbf{DX} + \mathbf{v}^i \end{aligned} \quad (17)$$

where $\mathbf{D} = \mathbf{HA}_c\mathbf{H}$ is the channel frequency response of DHT-based MCM system. As DHT is a real-valued transform, we express the equivalent baseband of the complex channel $\mathbf{A}_c$ as $\mathbf{A}_c^R + \boldsymbol{j}\mathbf{A}_c^I$. According to (16), we have

$$\begin{aligned} \mathbf{D} = \mathbf{HA}_c\mathbf{H} &= \mathbf{H}(\mathbf{A}_c^R + \boldsymbol{j}\mathbf{A}_c^I)\mathbf{H} \\ &= (\mathrm{Re}\{\boldsymbol{\Lambda}^R\} + \mathbf{J}_n\mathrm{Im}\{\boldsymbol{\Lambda}^R\}) \\ &\quad + \boldsymbol{j}(\mathrm{Re}\{\boldsymbol{\Lambda}^I\} + \mathbf{J}_n\mathrm{Im}\{\boldsymbol{\Lambda}^I\}), \end{aligned} \quad (18)$$

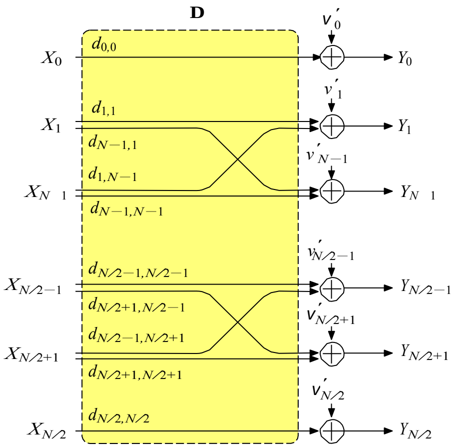

Fig. 2. Equvalient DHT-based MCM channel model in the frequency domain

where

$$\mathbf{\Lambda}^R = \mathbf{F}\mathbf{A}_c^R\mathbf{F}^H = \mathrm{diag}\{\lambda^R_k\}$$
$$\mathbf{\Lambda}^I = \mathbf{F}\mathbf{A}_c^I\mathbf{F}^H = \mathrm{diag}\{\lambda^I_k\}, \qquad 0 \le k \le N-1$$

Conventionally, FEQ can be applied to obtain an estimate of the transmitted symbol vector by

$$\hat{\mathbf{X}} = \mathbf{E}\mathbf{Y} = \mathbf{X} + \mathbf{v}^i$$

with ZF or MMSE coefficients as follows:

$$\begin{cases} \mathbf{E}_{ZF} = \mathbf{D}^{-1} \\ \mathbf{E}_{MMSE} = \mathbf{D}^H(\mathbf{D}\mathbf{D}^H + N_0\mathbf{I}_N)^{-1} \end{cases}. \tag{19}$$

An estimated bit sequence $\hat{\mathbf{b}}$ is finally recovered by feeding $\hat{\mathbf{X}}$ into a symbol to bit demapper.

B. Proposed Pairwise Detection Method

Upon examining the channel frequency response matrix $\mathbf{D}$ in (18), we can find that the subcarriers with index 0 and $N/2$ are independent with any other subcarriers and all other subcarriers coupled in pairs, therefore, we can decouple the subcarriers, this results in an equivalent channel model in the frequency domain as illustrated in Fig. 2.

The conventional equalization approach can be applied to the independent subcarriers for obtaining optimal solution. However, the inherent ICI resides in all other subcarriers due to coupling effect on mirror-symmetrical peers can not be eliminated by the conventional equalization approaches. This inevitably degrades system performance. We derive an optimal maximum likelihood detection (MLD) on a coupled pair basis for the proposed system.

Suppose subcarriers with index k and $\bar{k}$ are in a mirror-symmetrical pair, where $2 \le k \le N/2-1$, $\bar{k} = (N-k) \mod N$. The channel matrix $\mathbf{D}$ can be decoupled into independent 2×2 matrices $\{\mathbf{D}^P_1, \mathbf{D}^P_2, \ldots, \mathbf{D}^P_{N/2-1}\}$ where

$$\mathbf{D}_k^P = \begin{bmatrix} d_{k,k} & d_{k,\bar{k}} \\ d_{\bar{k},k} & d_{\bar{k},\bar{k}} \end{bmatrix}. \tag{20}$$

According to Eq. (17), we have

$$\mathbf{Y}_k^P = \mathbf{D}_k^P\mathbf{X}_k^P + \mathbf{v}_k^{iP} \tag{21}$$

where $\mathbf{Y}_k^P = [Y_k, Y_{\bar{k}}]^T$, $\mathbf{X}_k^P = [X_k, X_{\bar{k}}]^T$ and $\mathbf{v}_k^{iP} = [v^i_k, v^i_{\bar{k}}]^T$. The optimal solution to the estimated transmitted symbol vector $\hat{\mathbf{X}}^P_k = [\hat{X}_k, \hat{X}_{\bar{k}}]^T$ under ML criterion can be expressed as

$$\hat{\mathbf{X}} = \arg\min_{s,\bar{s}\in S} \|\mathbf{Y}^P_k - \mathbf{D}^P_k\mathbf{s}^P_k\|^2 \tag{22}$$

where $\mathbf{s}^P_k = [s, \bar{s}]^T$ and $\|\mathbf{Y}^P_k - \mathbf{D}^P_k\mathbf{s}^P_k\|^2$ corresponds to ML matrix. The ML approach achieves the optimal performance like the maximum a posteriori (MAP) detection when all symbols are equally likely to be transmitted. However the complexity increases quadratically as modulation order increases. The required number of ML metric calculation is M^2 for M-ary QAM.

We further derive soft information of bits for the pair MLD in the rest of the section. Since $v^i_k, v^i_{\bar{k}}$ are Gaussian distributed with zero mean and variance of N_0, the probability of received symbol pair $\mathbf{Y}^P_k$ given the transmitted pair $\mathbf{X}^P_k$ can be expressed as

$$p(\mathbf{Y}^P_k|\mathbf{X}^P_k) = \frac{1}{\pi N_0}\exp\left(\frac{-\|\mathbf{Y}^P_k - \mathbf{D}^P_k\mathbf{X}^P_k\|^2}{N_0}\right). \tag{23}$$

The soft information of k^{th} bit of the symbol on the k^{th} subcarrier is expressed by the mean of log-likelihood ratio (LLR) as

$$L_{k,k} = \log\frac{p(b_{k,k}=1|\mathbf{Y}^P_k)}{p(b_{k,k}=0|\mathbf{Y}^P_k)} = \log\frac{\sum_{s\in S_k^{(1)}} p(s|\mathbf{Y}^P_k)}{\sum_{s\in S_k^{(0)}} p(s|\mathbf{Y}^P_k)}, \tag{24}$$

where $S_k^{(1)}$ and $S_k^{(0)}$ are partitions of the set S divided according to the k^{th} bits of the elements being 1 or 0. Applying law of total probability and Bayes' rule successively to (24), we have

$$\begin{aligned} L_{k,k} &= \log\frac{\sum_{s\in S_k^{(1)}}\sum_{\bar{s}\in S} p(\mathbf{s}^P_k|\mathbf{Y}^P_k)}{\sum_{s\in S_k^{(0)}}\sum_{\bar{s}\in S} p(\mathbf{s}^P_k|\mathbf{Y}^P_k)} \\ &= \log\frac{\sum_{s\in S_k^{(1)}}\sum_{\bar{s}\in S} p(\mathbf{Y}^P_k|\mathbf{s}^P_k)}{\sum_{s\in S_k^{(0)}}\sum_{\bar{s}\in S} p(\mathbf{Y}^P_k|\mathbf{s}^P_k)}. \end{aligned} \tag{25}$$

Substituting (23) into (25), we have

$$L_{k,k} = \log\frac{\sum_{s\in S_k^{(1)}}\sum_{\bar{s}\in S}\exp\left(\frac{-\|\mathbf{Y}^P_k - \mathbf{D}^P_k\mathbf{s}^P_k\|^2}{N_0}\right)}{\sum_{s\in S_k^{(0)}}\sum_{\bar{s}\in S}\exp\left(\frac{-\|\mathbf{Y}^P_k - \mathbf{D}^P_k\mathbf{s}^P_k\|^2}{N_0}\right)}. \tag{26}$$

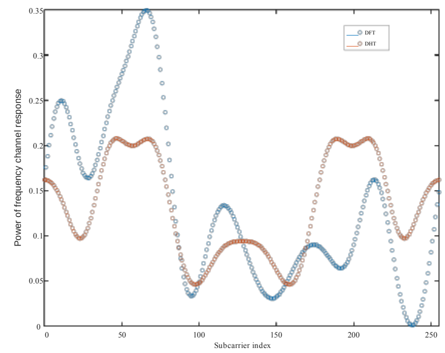

Fig. 3. Channel power gain comparison between DHT-based MCM and DFT-based MCM

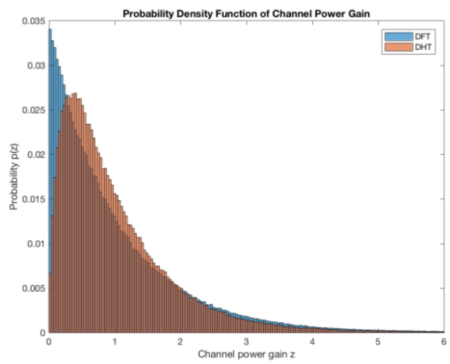

Fig. 4. PDF of channel power gain for DHT-based MCM and DFT- based MCM

Applying the log-sum-exp approximation identity: $\log \sum_i \exp(\varphi_i) \approx max(\varphi_i)$, we obtain

$$L_{k,k} = -\frac{1}{N_0}\Big(\max_{s \in S_k^{(1)}, s \in S} \|\mathbf{Y}_k^P - \mathbf{D}_k^P \mathbf{s}_k^P\|^2 - \max_{s \in S_k^{(0)}, s \in S} \|\mathbf{Y}_k^P - \mathbf{D}_k^P \mathbf{s}_k^P\|^2 \Big). \quad (27)$$

Similarly, the soft information of the k^{th} bit of the symbol on the $\bar{k}^{th}$ subcarrier can be obtained by simply swapping s and s^i in Eq. (27). If hard bits are needed due to the system configuration, they can be obtained through the following decision criterion:

$$b_k = \begin{cases} 1, & \text{if } L_k > 0 \\ 0, & \text{if } L_k \leq 0 \end{cases}. \quad (28)$$

IV. Numerical Results

In this section, we will compare the BER performance of a 256-subcarrier DFT-based MCM and a 256-subcarrier DHT-based MCM system in the presence of a multipath fading channel by the means of Monte Carlo simulation. The employed fading channel is the one adopted by the IEEE 802.11 working group [14] with

$$h_l = N(0, 0.5\sigma_l^2) + jN(0, 0.5\sigma_l^2),$$
$$\sigma_l^2 = \sigma_0^2 \exp(-lT_s/T_{RMS})$$
$$\sigma_0^2 = 1 - \exp(-T_s/T_{RMS}),$$

where h_k is the complex channel gain of the kth tap, T_{RMS} is the RMS delay spread of the channel, T_s is the sampling period, σ_0^2 is chosen so that the condition $\sum_l \sigma_l^2 = 1$ is satisfied to ensure same average received power. The number of samples to be taken in the impulse response should ensure sufficient decay of the impulse response tail, e.g., $l_{\max} = 10 \times T_{RMS}/T_s$. The RMS delay spread is set to be $T_{RMS} = 50ns$ and the sampling rate is $f_s = 1/T_s = 100$ MHz.

A. Lower Probability of Deep Fading

Based on (5) and (18), we can express the channel power gain on the k^{th} subcarrier for DFT-based and DHT-based MCM respectively as

$$\mathbf{E}\{Z_k^F\} = \mathbf{E}\{[\mathrm{Re}\{\lambda_k\}]^2 + [\mathrm{Im}\{\lambda_k\}]^2\}$$
$$\mathbf{E}\{Z_k^H\} = \mathbf{E}\{[\mathrm{Re}\ \lambda_k^R]^2 + [\mathrm{Im}\ \lambda_{\bar{k}}^R]^2 + [\mathrm{Re}\ \lambda_k^I]^2 + [\mathrm{Im}\ \lambda_k^I]^2\}, \quad (29)$$

where $\mathbf{E}\{.\}$ is expectation function.

According to the conjugate symmetry property of Fourier transform with real-valued input, we have $\lambda_k^R = (\lambda_{\bar{k}}^R)^*$ and $\lambda_k^I = (\lambda_{\bar{k}}^I)^*$ where the k^{th} and $\bar{k}^{th}$ subcarriers are in a mirror-symmetric pair. This indicates that the channel power gains on mirror-symmetric subcarriers are equally shared $\mathbf{E}\{Z_k^H\} = \mathbf{E}\{Z_{\bar{k}}^H\}$ as shown in Fig.3, while channel power gains in the DFT-based system do not have this property. As a result, deep fading happens in DHT-based MCM only when both subcarriers in a mirror-symmetric pair experiences deep fading in DFT-based MCM, which indicates a lower probability of deep fading in DHT-Based MCM. Fig. 4 plots the probability density function (PDF) of a channel power gain for DHT-based MCM and DFT-based MCM. It can be seen with DHT-based MCM that the probability of channel gain in deep fading region is lower when $z < 1/SNR$, where SNR denotes the signal to noise power ratio.

B. BER performance

The BER comparisons between two systems are based on the same signal-to-noise ration per bit, E_b/N_0. To ensure the reliability of the computer simulation, 10^6 OFDM symbols are generated to obtain each BER values in Figs. 5 and 6. Other simulation parameters adopted are listed in the table below:

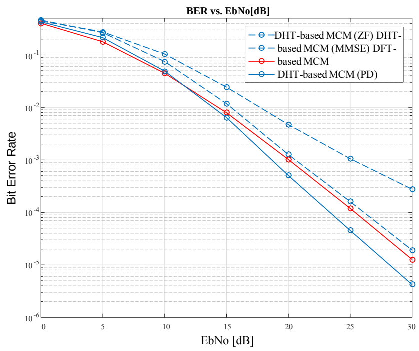

Fig. 5. BER performance comparison among different equalization and detection methods for DHT-based MCM (16-QAM, channel coding and soft demapping).

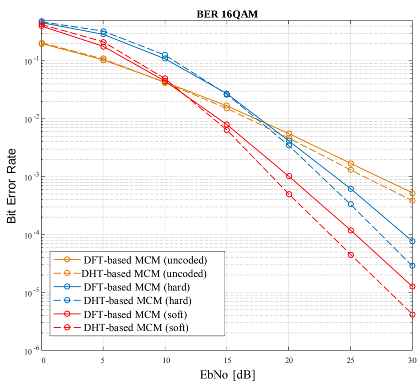

Fig. 6. BER performance comparison between DHT-based MCM and DFT-based MCM

TABLE I
SIMULATION PARAMETERS

Parameter	Value
Modulation mapper	64-QAM
Number of subcarriers (N)	256
Number of data blocks per frame	6
CP length (N_{cp})	12
Channel encoder/decoder	Convolutional/Viterbi
Polynomial generator	(7,[133,171])
Fading channel	802.11 fading channel [14]
Number of channel taps	11

Fig.5 shows a BER comparison between among equalization and detection methods, ZF/MMSE/pairwise detection (PD), for DHT-based MCM with channel coding and soft demapping employed in the simulation. We can observe that MMSE outperforms ZF significantly, however both of them can not match the BER performance in DFT- based MCM. PD as an optimal solution eliminating the inherent ICI outperforms MMSE by approximately 4dB at a bit error rate of 2×10^{-5} and it can make DHT-based MCM reach a better performance than DFT-based MCM. We will explore the BER performance comparison between the two systems in detail in Fig. 6.

Fig. 6 compares BER performance for three different channel coding configurations (uncoded, hard coded and soft coded) between two systems when PD is employed in the DHT-based system. The DHT-based MCM offers consistent performance improvement over DFT-based MCM in all the three configurations. Specifically, at a BER of 10^{-5}, approximately 3dB gain is observed.

V. CONCLUSION

In this paper, we have investigated the interference effect on mirror-symmetrical subcarriers in the frequency domain channel response. We have also proposed a DHT-based MCM transceiver structure, which supports transmitting complex symbols and a pairwise ML detection method for the system to eliminate the inherent ICI and to achieve channel diversity gain. Simulation results have shown the proposed scheme achieves a considerable performance gain as compared with the traditional DFT-based systems.

REFERENCES

[1] A. Goldsmith, *Wireless communications*. Cambridge Univ. Press, 2005.

[2] S. Weinstein and P. Ebert, "Data transmission by frequency-division multiplexing using the discrete Fourier transform," *IEEE Trans. Commun. Techno.*, vol. 19, no. 5, pp. 628–634, Oct. 1971.

[3] L. Zhang, A. Ijaz, P. Xiao, A. Quddus, and R. Tafazolli, "Subband filtered multi-carrier systems for multi-service wire- less communications," *IEEE Trans. Wireless Commun.*, vol. 16, no. 3, pp. 1893–1907, Mar. 2017.

[4] L. Zhang, P. Xiao, A. Ijaz, and R. Tafazolli, "Multi-service system: An enabler of flexible 5G air-interface," *IEEE Commun. Mag.*, pp. 1–9, 2017, to apper.

[5] P. Tan and N. C. Beaulieu, "A comparison of DCT-based OFDM and DFT-based OFDM in frequency offset and fading channels," *IEEE Trans. Commun.*, vol. 54, no. 11, pp. 2113–2125, Nov. 2006.

[6] R. Merched, "On OFDM and single-carrier frequency-domain systems based on trigonometric transforms," *IEEE Signal Pro- cess. Lett.*, vol. 13, no. 8, pp. 473–476, Aug. 2006.

[7] C.-L. Wang, C.-H. Chang, J. L. Fan, and J. M. Cioffi, "Discrete Hartley transform based multicarrier modulation," in *Proc. IEEE ICASSP, Istanbul, Turkey*, vol. 5, Jun. 2000, pp. 2513–2516.

[8] C. K. Jao, S. S. Long, and M. T. Shiue, "On the DHT-based multicarrier tranceiver over multipath fading channel," in *in Proc. IEEE PIMRC, Tokyo, Japan,*, Sept 2009, pp. 1662–1666.

[9] R. N. Bracewell, "The fast Hartley transform," *Proc. IEEE*, vol. 72, no. 8, pp. 1010–1018, Aug. 1984.

[10] H. S. Hou, "The fast Hartley transform algorithm," *IEEE Transactions on Computers*, vol. C-36, no. 2, pp. 147–156, Feb 1987.

[11] C. F. Wu, M. T. Shiue, and C. K. Wang, "DHT-based frequency-domain equalizer for DMT systems," in *Proc. European Signal Process. Conf., Antalya, Turkey*, Sept 2005, pp. 1–4.

[12] D. Wang, D. Liu, F. Liu, and G. Yue, "A novel DHT-based ultra-wideband system," in *Proc. IEEE Int. Symp. Commun. Inf. Techno., Beijing, China*, vol. 1, Oct 2005, pp. 672–675.

[13] P. J. Davis, *Circulant Matrices*. New York, USA: Wiley, 1979. [14] B.O'Hara and A. Petrick, *The IEEE 802.11 Handbook: A Designers Companion, 2nd Ed.* New York, USA: IEEE Press and Willy, 2011.